

## ORIGINAL ARTICLE

# Links between viral and prokaryotic communities throughout the water column in the (sub)tropical Atlantic Ocean

Daniele De Corte<sup>1,2</sup>, Eva Sintes<sup>1</sup>, Christian Winter<sup>3</sup>, Taichi Yokokawa<sup>1</sup>, Thomas Reinthaler<sup>3</sup> and Gerhard J Herndl<sup>1,3</sup>

<sup>1</sup>Department of Biological Oceanography, Royal Netherlands Institute for Sea Research (NIOZ), Den Burg, The Netherlands; <sup>2</sup>Center for Ecological and Evolutionary Studies, University of Groningen, Haren, The Netherlands and <sup>3</sup>Faculty Center of Ecology, Department of Marine Biology, University of Vienna, Vienna, Austria

**Viral and prokaryotic abundance, production and diversity were determined throughout the water column of the subtropical Atlantic Ocean to assess potential variations in the relation between viruses and prokaryotes. Prokaryotic abundance and heterotrophic activity decreased by one and three orders of magnitude, respectively, from the epi- to the abyssopelagic layer. Although the lytic viral production (VP) decreased with depth, lysogenic VP was variable throughout the water column and did not show any trend with depth. The bacterial, archaeal and viral community composition were depth-stratified as determined by the automated ribosomal intergenic spacer analysis, terminal-restriction fragment length polymorphism and randomly amplified polymorphic DNA-PCR, respectively. Generally, the number of operational taxonomic units (OTUs) did not reveal consistent trends throughout the water column. Viral and prokaryotic abundance were strongly related to heterotrophic prokaryotic production, suggesting similar linkage strength between the viral and prokaryotic communities from the lower epi- to the abyssopelagic layer in the Atlantic Ocean. Strikingly, the prokaryotic and viral parameters exhibited a similar variability throughout the water column down to the abyssopelagic layers, suggesting that the dark ocean is as dynamic a system as is the lower epipelagic layer. It also indicates that viruses are apparently having a similar role for prokaryotic mortality in the dark oceanic realm as in surface waters. The more than twofold increase in bacterial OTUs from 2750 m depth to >5000 m depth and the concurrent decrease in viral OTUs, however, suggests that viruses might exhibit a wider host range in deep waters than in surface waters.**

*The ISME Journal* (2010) 4, 1431–1442; doi:10.1038/ISMEJ.2010.65; published online 20 May 2010

**Subject Category:** microbial ecology and functional diversity of natural habitats

**Keywords:** viruses; prokaryotes; romanche fracture zone; atlantic; deep sea

## Introduction

Viruses have a key role in the biogeochemical processes of the ocean (Fuhrman, 1999; Suttle, 1999; Wilhelm and Suttle, 1999). Marine viruses may also control prokaryotic abundance and diversity (Thingstad and Lignell, 1997; Weinbauer and Rassoulzadegan 2004; Breitbart *et al.*, 2008) and are agents of transfer of genetic material between microorganisms (transduction and transformation; Fuhrman, 2000).

There are two main viral life strategies: lysogeny and lysis (Ackermann and DuBow, 1987). These different strategies may have a different impact

on the structure of the prokaryotic community. Lysogeny is considered to be an adaptation to low host abundance and/or activity because it has been reported to increase with depth, whereas the lytic cycle dominates at high host abundance and/or activity (Weinbauer *et al.*, 2003). Viruses are assumed to be host-specific (Ackermann and DuBow, 1987), however, some marine phages have been shown to exhibit a broad host range (Sullivan *et al.*, 2003; Sano *et al.*, 2004; Holmfeldt *et al.*, 2007). The viral infection rate, among other parameters, depends on the host abundance (Murray and Jackson, 1992). Thus, viruses are assumed to preferentially infect the winners in the competition for nutrients, which may or may not be the most abundant members of the community but most likely the most active ones (Thingstad and Lignell, 1997; Thingstad, 2000; Bouvier and del Giorgio, 2007).

Prokaryotic community composition can be determined using fingerprinting techniques such as

Correspondence: GJ Herndl, Department of Biological Oceanography, Center of Ecology, University of Vienna, Althanstrasse 14, Vienna 1090, Austria.

E-mail: gerhard.herndl@univie.ac.at

Received 5 February 2010; revised 13 April 2010; accepted 13 April 2010; published online 20 May 2010

terminal-restriction fragment length polymorphism (T-RFLP) and denaturing gradient gel electrophoresis targeting the 16S rRNA gene or automated ribosomal intergenic spacer analysis (ARISA) targeting the intergenic spacer (ITS) region in the rRNA operon. The composition of viral communities, representing the largest reservoir of genetic diversity in the ocean (Rohwer, 2003), is more difficult to determine because of the lack of universally conserved marker genes. Until recently, pulsed-field gel electrophoresis (PFGE) based on size fractionation of viral double-stranded DNA was the main tool to investigate viral community composition (Klieve and Bauchop, 1988; Wommack *et al.*, 1999b). The recently introduced randomly amplified polymorphic DNA (RAPD)-PCR approach allows one to resolve the viral community structure at a higher resolution than PFGE does (Winget and Wommack, 2008).

The aim of this study was to determine the distribution of prokaryotic and viral abundance, and production and community composition throughout the water column in the (sub)tropical Atlantic Ocean from the epi- to the abyssopelagic realm (from 100 to 7000 m depth). Thus far, most of the studies on the interaction and relation of viral to prokaryotic abundance, production and community composition have been performed in surface waters. The recently reported increase in the ratio of viral to prokaryotic abundance from surface waters to bathypelagic layers in the Atlantic (Parada *et al.*, 2007) in combination with the low growth rates of the bulk bathy- and abyssopelagic prokaryotic communities indicates, however, that the interactions between viruses and prokaryotes in the dark realm of the ocean might be fundamentally different from those in surface waters (Herndl *et al.*, 2008). Thus, we specifically focused on indications of potential changes in the interaction between viruses and prokaryotes from the base of the epipelagic zone to the abyssopelagic layers.

## Materials and methods

### *Study area and sampling*

Water samples were obtained at 37 stations from the epi- (~100 m depth) to the abyssopelagic layer (to 7000 m depth) (Figure 1) during the ARCHIMEDES-III cruise in the (sub)tropical Atlantic Ocean aboard the R/V *Pelagia* (December 2007/January 2008). Sampling was performed with a CTD (conductivity-temperature-depth) rosette sampler equipped with 12-l Niskin bottles (General Oceanics, Miami, FL, USA). The Niskin bottles were flushed with bleach and rinsed with ambient seawater before collecting the samples by deploying them to 1000 m depth.

### *Prokaryotic and viral abundance*

Prokaryotic and viral abundance were determined by flow cytometry (Del Giorgio *et al.*, 1996; Brussaard, 2004). For enumerating prokaryotes, 2 ml

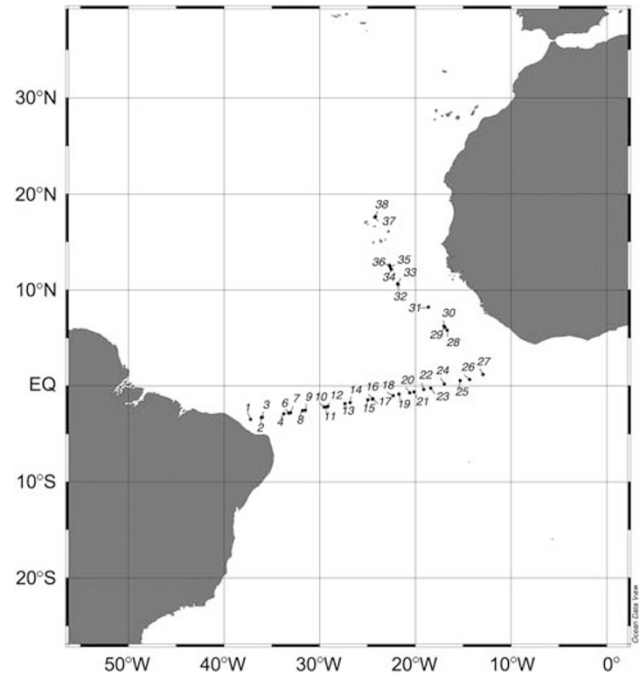


**Figure 1** Sampling sites indicated by full circles during the ARCHIMEDES III cruise in the (sub)tropical Atlantic Ocean (water samples were not collected at St. 5).

samples were fixed with glutaraldehyde (0.5% final concentration), shock-frozen in liquid N<sub>2</sub> and kept at -80 °C until analysis. Before flow cytometric analysis, samples were thawed to room temperature and 0.5 ml subsamples were stained with SYBR Green I in the dark for 10 min. Subsequently, 1 × 10<sup>5</sup> ml<sup>-1</sup> of 1 μm fluorescent latex beads (Molecular Probes, Invitrogen, Carlsbad, CA, USA) were added to each sample as internal standard. The prokaryotes were enumerated on an FACScalibur flow cytometer (Becton Dickinson, Franklin Lakes, NJ, USA) by their signature in a plot of green fluorescence versus side scatter.

Viral abundance was measured by flow cytometry after SYBR Green I staining (Brussaard, 2004). Briefly, 2 ml samples were fixed with glutaraldehyde (0.5% final concentration), held at 4 °C for 10–30 min, frozen in liquid N<sub>2</sub> and subsequently stored at -80 °C until analysis. Before analysis, samples were thawed and 0.5 ml subsamples were stained in the dark with SYBR Green I (Molecular Probes) at a final concentration of 0.5 × of the manufacturer's stock solution at 80 °C for 10 min. Subsequently, 1 μm fluorescent latex beads (Molecular Probes) (10<sup>5</sup> ml<sup>-1</sup>) were added to the samples as internal standard. The virus-like particles (VLP) were enumerated on an FACScalibur flow cytometer (Becton Dickinson) by their signature in a plot of green fluorescence versus side scatter.

### *Heterotrophic prokaryotic activity*

Prokaryotic leucine incorporation was measured on triplicate 10–40 ml samples (depending on the

expected activity) and on triplicate formaldehyde-killed blanks (Simon and Azam, 1989). The samples and blanks were inoculated with 5 nM  $^3\text{H}$ -leucine (final concentration, specific activity 160 Ci mmol $^{-1}$ , Amersham, GE Healthcare, Buckinghamshire, UK) and incubated in the dark at *in situ* temperature for 4–24 h depending on the expected activity. Subsequently, the samples were fixed with formaldehyde (2% final concentration), filtered onto 0.2  $\mu\text{m}$  polycarbonate GTTP filters (Millipore, Billerica, MA, USA) supported by Millipore HAWP filters, and rinsed three times with 10 ml of 5% ice-cold trichloroacetic acid. Thereafter, the filters were transferred into scintillation vials and dried at room temperature. Then, 8 ml of scintillation cocktail (Packard Filter Count, PerkinElmer, Waltham, MA, USA) was added to each vial and counted in a Tri-Carb 2910TR (PerkinElmer, Groningen, The Netherlands) liquid scintillation counter after 18 h. The obtained disintegrations per minute were converted to leucine incorporation rates, and prokaryotic carbon production was calculated from leucine incorporation rates using the conversion factor of 1.55 kg mol $^{-1}$  Leu incorporated (Simon and Azam, 1989). Prokaryotic cell abundance was converted into prokaryotic carbon biomass assuming a carbon content of 20 fg C per cell (Lee and Fuhrman, 1987). The turnover time of the heterotrophic prokaryotic community was calculated by dividing bulk prokaryotic biomass by prokaryotic carbon production.

#### *Viral production*

Viral production (VP) was measured by the dilution approach (Wilhelm *et al.*, 2002). Briefly, 50 ml of the prokaryotic concentrate obtained by 0.2  $\mu\text{m}$  tangential flow filtration (Vivascience, Sartorius Stedim Biotech, Aubagne Cedex, France) was added to 450 ml of virus-free filtrate produced from the same water sample using a 30 kDa molecular weight cut-off tangential flow filtration (Vivascience). This approach resulted in a prokaryotic abundance similar to *in situ* abundance. Subsamples were taken to enumerate prokaryotes and viruses at 7 h intervals over a time span of 72 h. The experiments were performed in duplicate at *in situ* temperature in the dark with and without the addition of mitomycin C (final concentration 5  $\mu\text{g ml}^{-1}$ ; Sigma, St Louis, MO, USA; Ortmann *et al.*, 2002). Mitomycin C was added to induce the lytic cycle of lysogenic viruses. VP was calculated as the slope of a first-order regression line of viral abundance versus incubation time for the samples showing a single peak in viral abundance (Wilhelm *et al.*, 2002). For samples with two peaks in viral abundance, the VP was calculated using the formula:

$$VP = [(V_{\max 1} - V_{\min 1}) + (V_{\max 2} - V_{\min 2})] / (t_{\max 2} - t_{\min 1})$$

where  $V$  = viral abundance and  $t$  = time and subscripts 1 and 2 refer to peaks 1 and 2 in viral abundance (Winter *et al.*, 2004a).

Lytic VP was obtained from incubations without the addition of mitomycin C. Lysogenic VP is the difference between the VP obtained in the mitomycin C-treated samples and the samples without mitomycin C.

#### *Viral community composition*

For the analysis of the viral community composition, one sample from each of the nine stations sampled in total for this parameter was collected. For the bathy- and abyssopelagic layers, 150 l, and for the epi- and mesopelagic layers, 70 l of water were collected and pre-filtered through a 0.22  $\mu\text{m}$  polycarbonate filter (293 mm diameter, Whatman Nuclepore, Kent, UK). This 0.22  $\mu\text{m}$  filtrate was subsequently concentrated to a final volume of  $\sim 50$  ml by tangential flow filtration with a 30 kDa molecular weight cut-off (Vivascience) and stored at  $-80^\circ\text{C}$  until DNA extraction. The viral concentrate was further concentrated to a final volume of 200  $\mu\text{l}$  by centrifugation ( $5000 \times g$  for 20 min) with Amicon Ultra 30 kDa molecular weight cut-off spin filters (Millipore). DNA extraction was performed with QIAamp MinElute Virus Spin Kit (Qiagen, Hilden, German) using the protocol of the manufacturer. The extract was directly used as the PCR template. For RAPD-PCR, the primer CRA-22 (5'-CCGCAGCC AA-3') was used to amplify viroplankton DNA (Winget and Wommack, 2008; Wommack *et al.*, 1999b) in 50  $\mu\text{l}$  of PCR mixture. Only one primer was used in each reaction, which acted as the forward and reverse primer. Samples were amplified by an initial denaturation step at  $94^\circ\text{C}$  for 10 min, followed by 30 cycles of annealing at  $35^\circ\text{C}$  for 3 min, extension at  $72^\circ\text{C}$  for 1 min and denaturation at  $94^\circ\text{C}$  for 30 s. The cycle was completed by final extension at  $72^\circ\text{C}$  for 10 min, and then kept at  $4^\circ\text{C}$ . The quality of the RAPD-PCR products was checked on 2% agarose gel. The products were purified with the Quick PCR purification kit (Genscript, Piscataway, NJ, USA) and quantified with a Nanodrop spectrophotometer. Subsequently, the purified RAPD-PCR products were separated by electrophoresis with an Experion automated electrophoresis system (Bio-Rad, Hercules, CA, USA). The obtained image was analysed with Fingerprinting II software (Bio-Rad).

#### *Prokaryotic community composition*

Samples for prokaryotic community composition were taken at the same depths and stations as those for viral community composition. Ten litres of seawater was filtered through a 0.22  $\mu\text{m}$  Sterivex filter. Subsequently, 1.8 ml of lysis buffer (40 mM EDTA, 50 mM Tris-HCL, 0.75 M sucrose) was added and the filters were stored at  $-80^\circ\text{C}$  until further processing. DNA extraction was performed using a Mega Kit extraction (MoBio Laboratories, Carlsbad, CA, USA) using the manufacturer's protocol. DNA extracts were concentrated ( $\sim 10$  times) with a Centricon device (Millipore).

For archaeal community analysis, PCR and T-RFLP were used. PCR conditions and chemicals were applied as described by Moeseneder *et al.* (2001a). One millilitre of the DNA extract was used as a template in a 50 ml PCR mixture. The primers for PCR were the Archaea-specific primer pair 21F-FAM end-labelled with phosphoramidite fluorochrome 5-carboxyfluorescein and 958R-JOE with 6-carboxy-4',5'-dichloro-2',7'-dimethoxyfluorescein (DeLong, 1992). Samples were amplified by an initial denaturation step at 94 °C for 3 min, followed by 35 cycles of denaturation at 94 °C for 1 min, annealing at 55 °C for 1 min, and an extension at 72 °C for 1 min. Cycling was completed by final extension at 72 °C for 7 min. The PCR products were run on 1.0% agarose gels. The gel was stained with a working solution of SYBR Gold, the obtained bands excised, purified by Quick gel extraction kit (Genscript) and quantified using a Nanodrop spectrophotometer. Fluorescently labelled PCR products were digested at 37 °C overnight. Each reaction contained 30 ng of cleaned PCR product, 5 U of the tetrameric restriction enzyme *HhaI*, and the respective buffer (Fermentas Life Science, Burlington, Canada) filled up to a final volume of 50 µl with ultra-pure water (Sigma). The restriction enzyme was heat-inactivated and precipitated by adding 4.5 µl linear polyacrylamide (prepared with acrylamide, tetramethylethylenediamin (TEMED) and ammonium persulphate (APS) in Tris-EDTA buffer) solution to 100 µl of 100% isopropanol. The samples were stored at room temperature for 15 min and subsequently centrifuged at 15000 × g for 15 min. After removing the supernatant, the pellets were rinsed with 100 µl of 70% isopropanol and precipitated again by centrifugation (15 000 × g for 5 min). After removal of the supernatant, the samples were dried in the cyclor at 94 °C for 1 min and stored at -20 °C.

The pellet was resuspended in 2 µl of ultra-clean water (Sigma), and denatured after the addition of 7.8 µl of Hi-Di formamide (highly deionized formamide for capillary electrophoresis) (Applied Biosystems, Foster City, CA, USA) at 94 °C for 3 min. Each sample contained 0.2 µl GeneTrace 1000 (X-Rhodamine labelled) marker (Applied Biosystems). Fluorescently labelled fragments were separated and detected using an ABI Prism 310 capillary sequencer (Applied Biosystems) run under GeneScan mode (Moeseneder *et al.*, 2001a). The size of the fluorescently labelled fragments was determined by comparison with the internal size standard. Injection was performed electrokinetically at 15 kV for 15 s (adjustable), and the runs were conducted at 15 kV and 60 °C within 38 min.

The output from the ABI Genescan software was transferred to the Fingerprinting II software (Bio-Rad) to calculate the area of the peaks and for standardizing them by the size marker. The obtained matrix was analysed using Primer software (Primer-E, Ivybridge, UK) to determine the similarity between T-RFLP patterns obtained from different samples.

To assess bacterial community composition, ARISA-PCR was used following the method of Borneman and Triplett (1997) with modifications. One µl of the DNA extract was used as a template in a 40 µl PCR mixture. The primers used were ITSf, 5'GTTCGTAACAAGGTAGGCCGTA-3' and ITSr eub, 5'-GCCAAGGCATCCACC-3' (Cardinale *et al.*, 2004); the primer ITSf was end-labelled with phosphoramidite fluorochrome 5-carboxyfluorescein dye 5-FAM. Samples were amplified by an initial denaturation step at 94 °C for 2 min, followed by 32 cycles of amplification at 94 °C for 15 s, 55 °C for 30 s, and 72 °C for 3 min and a final extension of 72 °C for 9 min. Five µl of PCR products were run on 2.0% agarose gels to check the quality of the products. The PCR products were purified with the Quick Clean PCR product purification kit (Genscript) and quantified using a Nanodrop spectrophotometer. Fluorescently labelled fragments (8 ng µl<sup>-1</sup> of sample) were separated and detected using an ABI Prism 310 capillary sequencer (Applied Biosystems) run under GeneScan mode (Kent *et al.*, 2004). The size of the fluorescently labelled fragments was determined by comparison with X-Rhodamine MapMarker 1000 (BIO Ventures, Murfreesboro, TN, USA) and the size standard. Injection was performed electrokinetically at 10 kV for 5 s (adjustable) and the run was conducted at 10 kV and 60 °C within 60 min.

Subsequent data processing was performed as described above for archaeal community analysis.

#### Statistical analysis

Spearman's rank correlation was performed to analyse the relationship between several measured parameters. The distance-based multivariate analysis for a linear model using forward selection (DISTLM forward) was performed to test the relationships between the bacterial, archaeal and viral communities and the biotic and abiotic environmental variability (Anderson *et al.*, 2004).

Linear regression analysis was used to predict the relationship between viral and bacterial abundance and the heterotrophic prokaryotic production. Analysis of variance (ANOVA on rank) was performed to test possible differences among depth layers and, when significant differences were observed, *post hoc* Dunn's test was also performed.

Mantel's test was used to test whether the differences in biotic and abiotic parameters were due to geographic distance. Correlation and linear regression analyses were performed with SigmaPlot 10.00 (Systat Software, Chicago, IL, USA), and Mantel's test was performed with Past 1.94a (Hammer *et al.*, 2001).

## Results

#### Physicochemical variables

The temperature decreased from the surface to the abyssopelagic waters (Table 1). The salinity varied



**Table 2** Lytic and lysogenic VP rates, percentage of lysogenic viral production versus total viral production and viral turnover time measured at different depths and at different stations during ARCHIMEDES III in the subtropical Atlantic Ocean

Depth (m)	Station	Lytic VP ( $\times 10^5 \text{ ml}^{-1} \text{ h}^{-1}$ )	Lysogenic VP ( $\times 10^5 \text{ ml}^{-1} \text{ h}^{-1}$ )	%		Turnover time (h)
				Lysogenic VP	VP	
250	St.19	6.871	0.183	3		1.9
450	St.38	0.417	0.248	37		13.3
700	St.34	0.946	0.023	2		7.9
1750	St.22	0.283	ND	ND		25.6
2750	St.27	0.085	0.003	3		47.8
2750	St.31	0.04	0.062	61		39.6
2750	St.37	0.398	0.093	19		9.4
4500	St.13	0.04	0.002	6		78
4500	St.18	0.185	0.02	10		21.4
7000	St.23	0.188	0.138	42		13.4

Abbreviations: ND, not detectable; VP, viral production.

with a high nucleic acid content generally increased with depth from the epipelagic to the abyssopelagic layer (ANOVA on ranks  $P < 0.001$ ), reaching 79% at the deepest station (Tables 1 and 3, Supplementary Figure S3b).

Three different viral populations were distinguished on the basis of their fluorescence signal (Table 1, Supplementary Figure S4a). The high fluorescence fraction of the viral community ranged from 6% to 24% of total abundance with generally higher values in the epipelagic and abyssopelagic waters. It decreased significantly from the pelagic layers to the meso- and bathypelagic layers (ANOVA on ranks  $P < 0.001$ , *post hoc* Dunn's tests  $P < 0.05$ ) (Tables 1 and 3, Supplementary Figure S4b). The medium fluorescence fraction comprised on average  $79 \pm 4\%$  with no significant trend with depth (Tables 1 and 3, Supplementary Figure S4c). The low fluorescence population ranged from 3% to 29%, again without a specific depth-related trend (Tables 1 and 3, Supplementary Figure S4d).

Viral production was determined 10 times in total, at nine stations and 8 depths (Table 2). Lytic VP decreased linearly from about  $6.8 \times 10^5$  VLP per ml per h in the epipelagic layer to  $0.18 \times 10^5$  VLP per ml per h in the abyssopelagic realm (Tables 2 and 3). The lysogenic VP showed no clear trend with depth (Table 2). The total viral turnover time was calculated as the ratio between viral abundance and total (lytic plus lysogenic) VP. Total viral turnover time ranged between 2 h and 3 days without any clear depth-related trend (Table 2).

No significant differences over geographic distance at specific depths were found for the prokaryotic and viral abundance and the heterotrophic prokaryotic production.

#### *Viral and prokaryotic community composition*

The RAPD-PCR pattern of the viral community revealed in total 24 operational taxonomic units (OTUs) ranging from 182 to 1157 bp (Figure 2a). The

**Table 3** Results of Spearman's rank correlation coefficient test performed to determine the variation of the prokaryotic and viral parameters versus depth

	Depth		
	$r_s$	P-value	N
PA	-0.948	<0.0001	150
PHP	-0.910	<0.0001	150
Spec Leu	-0.820	<0.0001	150
VLP	-0.788	<0.0001	150
VPR	0.876	<0.0001	150
%HNA	0.598	<0.0001	150
VLP% High	-0.174	0.003	150
VLP% Medium	-0.030	0.716	150
VLP% Low	0.254	0.001	150
LyticVP	-0.683	0.036	10
LysogenicVP	-0.400	0.264	9

Abbreviations: LyticVP, total Lytic viral production; LysogenicVP, total lysogenic viral production; N, number of samples; PA, prokaryotic abundance; PHP, bulk leucine incorporation rate; Spec Leu, cell-specific leucine incorporation rate; VLP, virus-like particles; VPR, ratio of viral to prokaryotic abundance; %HNA, percentage of high nucleic acid prokaryotes; VLP %High, percentage of high fluorescence viral population; VLP %Medium, percentage of medium fluorescence viral population; VLP %Low, percentage of low fluorescence viral population. Relevant ( $-0.5 > r_s > 0.5$ ), statistically significant  $P < 0.05$ .

lowest number of OTUs (4) was found at St. 37 at 470 m depth, and the highest (17 OTUs) at St. 7 at 2750 m depth. The OTUs 1037 and 686 bp were detected in all the samples, whereas six OTUs were detected only once (Figure 2a). Jaccard similarity analysis of the viral community revealed a bathy-abyssopelagic cluster (1750–5200 m depth), whereas the mesopelagic viral communities were characterized by generally low similarity (Figure 2b).

The ARISA pattern of the bacterial community revealed in total 142 OTUs on the ITS level, ranging from 86 to 761 bp fragments (Figure 3a). The lowest number of OTUs (23) was detected at St. 35 at 100 m depth, the highest (88) at St. 27 at 5200 m depth (Figure 3a). Only one fragment was detectable in all the samples (369 bp).

The T-RFLP pattern of the archaeal community revealed in total 10 OTUs on the 16S rDNA level, ranging from 72 to 919 bp fragments (Figure 4a). The lowest number of OTUs (2) was detected at St. 27 at 5200 m depth and the highest (8) at St. 35 at 100 m depth (Figure 4a). Two archaeal OTUs were present throughout the water column.

For the bacterial communities, the Jaccard similarity cluster analysis of the ARISA fingerprints revealed two distinct clusters: an epi-, mesopelagic cluster and a bathy-, abyssopelagic cluster (Figure 3b). For the archaeal communities, Jaccard cluster analysis of the T-RFLP pattern indicated a meso- and upper bathypelagic cluster and a bathy-, abyssopelagic cluster (Figure 4b). The archaeal community at 100 m and 5200 m depth were distinctly different from all the other samples (Figure 4b). Overall, the viral, bacterial and archaeal

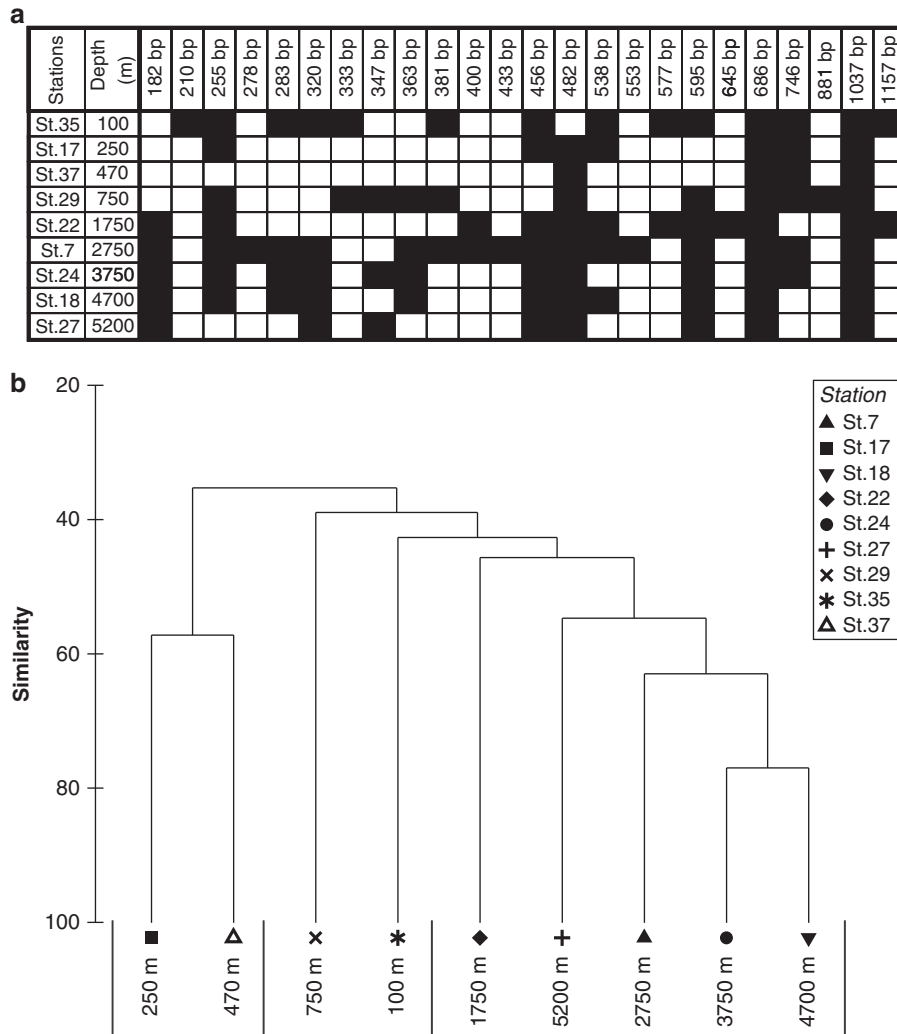


**Figure 2** Viral community composition as revealed by RAPD-PCR. Presence/absence (filled/open squares, respectively) of viral OTUs at different stations and depths (a). Clustering of samples from different depths based on the Jaccard similarity matrix obtained from the presence/absence pattern of the viral OTUs (b).

community composition were not significantly related to any of the environmental variables measured (DISTLM test,  $P > 0.1$ ).

The rank-frequency distribution of OTUs obtained for the viral community indicated that half of the OTUs appeared in less than 45% of the samples, whereas 10 OTUs were present in more than 50% of the samples (Figure 5). In contrast to the viral community, rare OTUs were more frequently encountered in the bacterial community (Figure 5). A high contribution (30% of the total number of OTUs) of unique bacterial OTUs was found in the oxygen minimum zone and at the deeper layer (20% of the total OTUs), whereas in the other depth layers the contribution of unique OTUs was limited to 1–4% of the total number of OTUs. Half of the bacterial OTUs were present in less than 22% of the samples and only 17% of the OTUs were present in more than 50% of the samples (Figure 5). The rank-frequency distribution of the archaeal community revealed that

half of the OTUs appeared in about 10% of the samples and only three OTUs (30%) were present in more than 50% of the samples (Figure 5).

The number of OTUs of archaea and viruses covaried with depth, decreasing from the subsurface waters to the upper mesopelagic and remaining fairly constant until 3000–4000 m depth and decreasing towards greater depths (Figure 6). The number of bacterial OTUs, however, increased from 3000 to 5200 m depth (Figure 6). The number of archaeal OTUs were positively correlated with the number of viral OTUs ( $r_s = 0.683$ ,  $P = 0.036$ ) and negatively correlated with the number of bacterial OTUs ( $r_s = -0.799$ ,  $P = 0.006$ ), whereas the number of viral and bacterial OTUs were not significantly correlated ( $r_s = -0.620$ ,  $P = 0.067$ ). The number of bacterial OTUs was negatively correlated with the archaeal OTUs even when the unique bacterial OTUs were excluded from the analysis. The 25 most abundant bacterial OTUs were evenly distributed



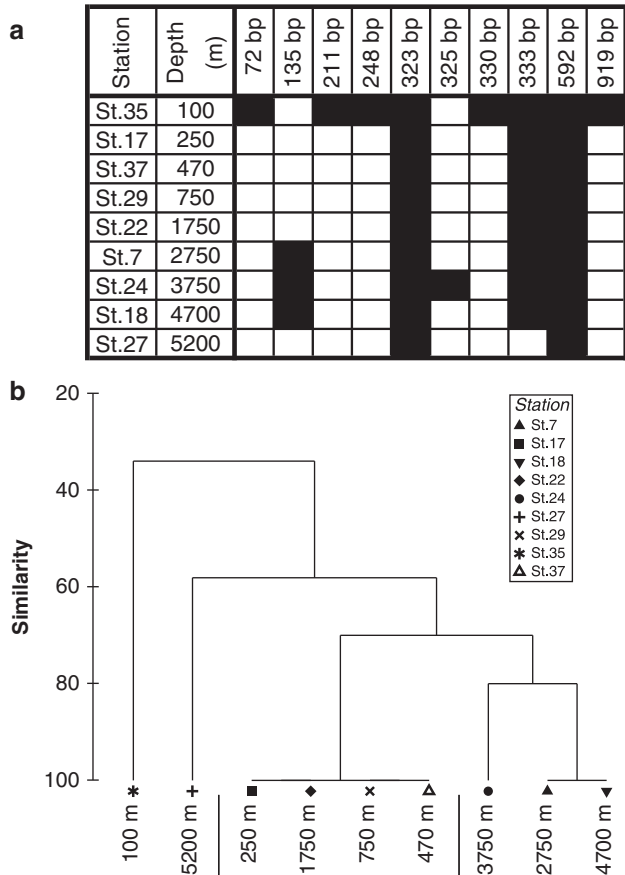


**Figure 4** Archaeal community composition as revealed by T-RFLP. Distribution (presence/absence) of archaeal OTUs at several stations and depths (a). Jaccard similarity matrices were used for cluster analysis based on T-RFLP fingerprints (b).

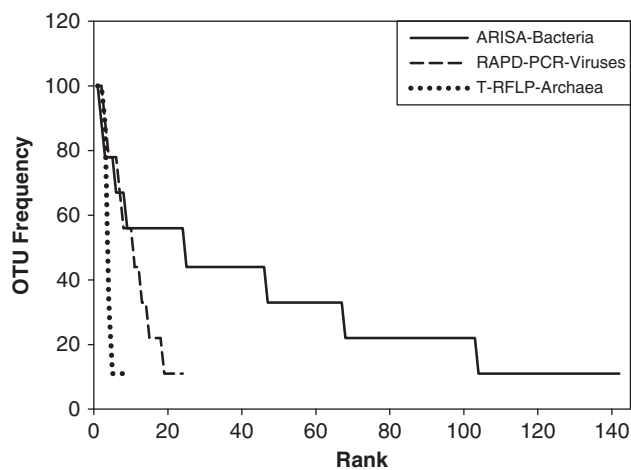


**Figure 5** Rank-frequency distribution of archaeal, bacterial and viral OTUs obtained from samples collected throughout the water column of the (sub)tropical Atlantic.

been reported previously (Allen and Bartlett, 2002; DeLong *et al.*, 2006; Reinthaler *et al.*, 2006). Lauro and Bartlett, 2008 showed that bathypelagic prokaryotes have generally a high copy number of rRNA

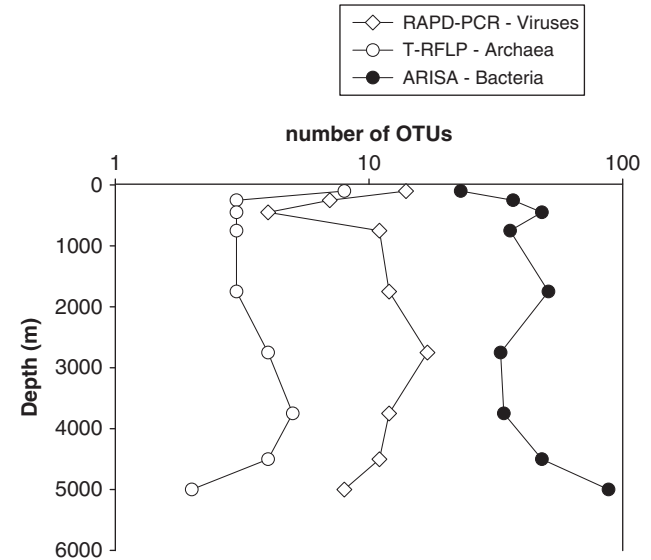


**Figure 6** Distribution of the number of OTUs of bacteria, archaea and viruses throughout the water column of the (sub)tropical Atlantic.

operons per genome and a larger intergenic region. In addition, a large number of genes involved in the synthesis of the polyunsaturated fatty acids is found in deep ocean bacteria (Allen *et al.*, 1999; Allen and Bartlett, 2002). Taken together, the notion emerges that deep-water prokaryotes are predominantly opportunists, presumably well adapted to a particle-attached life mode (Lauro and Bartlett, 2008; Aristegui *et al.*, 2009), which might explain the need for a larger genome size. Hence, the larger genome of prokaryotes in the deep waters corresponds to the higher fraction of high fluorescence viruses found in the abyssopelagic compared with the bathypelagic waters (Supplementary Figures S3b, Figure S4b).

#### Viral and heterotrophic prokaryotic production

The total viral turnover time in the meso- to abyssopelagic waters ranged between 2 h and 3 days without any clear depth-related trend (Table 2). Our calculated viral turnover time based on total VP is lower than the measured viral decay times (ranging between 11 and 39 days) for the North Atlantic Ocean (Parada *et al.*, 2007). These viral decay times reported by Parada *et al.* (2007) were derived from the decrease in viral abundance in 0.2 µm filtered seawater over time. It is very likely, however, that viruses are losing their infectivity before being undetectable by flow cytometry (Suttle, 2005). Hence, it is reasonable to assume that the viral turnover time based on VP is lower than the estimated viral decay time.

Viral production depends on the abundance of their hosts, ultimately determining the contact rate (Murray and Jackson, 1992). Weinbauer *et al.* (2003) proposed that the lysogenic cycle could be an adaptation to low host abundance and activity,

thus indicating a shift in the viral life strategy from lysis to lysogeny with increasing depth. The high percentage of lysogenic VP at some specific stations in the bathy- and abyssopelagic zones of the Atlantic corroborates these findings with values of lysogeny up to 61% of the total VP (Table 2). However, the lack of a specific trend with depth in lysogenic VP along with its considerable variability points to substantial patchiness in the interaction between viruses and prokaryotes in the bathy- and abyssopelagic realms.

Recently, Aristegui *et al.* (2009) reviewed deep-water prokaryotic abundance and activity and viral abundance and concluded that the variability in these parameters is as high in the deep ocean as in surface waters despite their decrease in average abundance by orders of magnitude over this depth range. In our study, heterotrophic prokaryotic activity decreased by three orders of magnitude from the epi- to the abyssopelagic layer and was generally similar to that reported for the deep waters of the southern region of the North Atlantic (Reinthal *et al.*, 2006). As mentioned above, heterotrophic prokaryotic activity was strongly related to viral abundance. This tight relation is therefore not restricted to coastal and neritic seas such as the North Sea (Winter *et al.*, 2005) and to surface waters but appears to hold also for the dark ocean down to the abyssopelagic layers. This close relation indicates that deep-water viruses are also predominantly prokaryophages.

The prokaryotic turnover time increased with depth from the epi- to the abyssopelagic layer, as shown in a recent review by Aristegui *et al.* (2009). The prokaryotic turnover time is based on the abundance of prokaryotes, enumerated by flow cytometry, and might include inactive, non-growing as well as dividing cells, whereas the viral turnover time is directly linked to the number of growing cells. This might, at least partly, explain the substantially higher (up to three orders of magnitude) viral than prokaryotic turnover time found in these deep waters.

#### *Links between viral and prokaryotic community composition*

Three different methods were used to determine the bacterial, archaeal and viral community composition targeting the ITS region, 16S rRNA and viral double-stranded DNA, respectively. ARISA and T-RFLP have been proven to be robust methods to determine the bacterial and archaeal community composition (Avaniss-Aghajani *et al.*, 1994; Fisher and Triplett, 1999). RAPD-PCR has only recently been introduced to assess viral community composition (Winget and Wommack, 2008) and represents a substantial improvement over PFGE because of its higher resolution.

The number of viral OTUs obtained in this study by RAPD-PCR is, however, substantially higher than

that obtained with PFGE in the deep Atlantic waters (Parada *et al.*, 2007), within the range reported for the Chesapeake Bay surface waters using PFGE (Wommack *et al.*, 1999a). The Jaccard cluster analysis of the RAPD-PCR pattern showed a clear stratification of the viral community with depth (Figure 2b) similar to that obtained for bacteria (Figure 3b).

Relatively low numbers of archaeal OTUs per sample (ranging from 2 to 8) were detected by T-RFLP (Figure 4a). The number of archaeal OTUs obtained in this study was lower than in previous studies on the deep tropical East Atlantic (Winter *et al.*, 2008) and in the deep Eastern Mediterranean Sea (Moeseneder *et al.*, 2001ab; De Corte *et al.*, 2009).

The Jaccard cluster analysis of the archaeal communities revealed two main clusters and generally a much higher similarity between samples than for bacteria (Figure 4b). In contrast to the archaeal community, relatively high numbers of bacterial OTUs were detected by ARISA. The large number of unique bacterial OTUs obtained on the ITS level is indicated by the long tail of the rank-frequency distribution of OTUs (Figure 5). The higher contribution of unique bacterial OTUs was found in the oxygen minimum zone and in the deepest layer sampled than in the other water layers, suggesting that these two layers might offer ecological niches different from the rest of the water column. The long tail in the rank-frequency distribution of bacterial OTUs was not found in the archaeal and viral community (Figure 5). The Jaccard cluster analysis of the bacterial community also indicates a clustering with depth (Figure 3b). The bacterial community richness, that is, the number of OTUs, was negatively related to prokaryotic abundance due to the high number of OTUs detected in the bathy- and abyssopelagic zones where prokaryotic abundance is low.

The viral and bacterial richness exhibited a contrasting pattern with depth (Figure 6). Although the richness of the bacterial community increased from about 3000–5000 m depth, the richness of the viral community decreased over this depth range (Figure 6). It is well documented that different fingerprinting techniques differ in their resolution resulting in different numbers of OTUs as shown for ARISA and T-RFLP (Danovaro *et al.*, 2006). Our observed trend in bacterial and viral communities with depth, however, is most likely independent of the different resolutions of the methods used assuming similar extraction and amplification efficiencies over the depth range of the water column sampled. Thus, the contrasting richness patterns between the bacterial and viral communities together with the lack of a decrease in viral abundance from the bathy- to abyssopelagic waters might indicate a wider host range of viruses in these deep waters than in the near-surface layers.

In summary, our data show a high variability of prokaryotic and viral abundance and production in

the bathy- and abyssopelagic zones, suggesting that the dark ocean is more heterogeneous than commonly assumed. Despite the heterogeneity in prokaryotic and viral abundance and production in the deep Atlantic, the archaeal, bacterial and viral community composition are stratified. Although viral turnover time does not exhibit a trend with depth in the deep ocean, bulk prokaryotic turnover time increases linearly with depth. Together with the increase in the virus-to-prokaryote ratio with depth, it might indicate that viruses very likely have a wider host range in the bathy- and abyssopelagic than in near-surface waters allowing them to infect the deep-water prokaryotic community characterized by low abundance but relatively high richness.

## Conflict of interest

The authors declare no conflict of interest.

## Acknowledgements

We thank the captain and crew of R/V Pelagia for their support and splendid atmosphere on board. ES was supported by the Dutch Science Foundation, TY was supported by the Japanese Society for the Promotion of Science (JSPS) Postdoctoral Fellowship for research abroad, DDC received a fellowship of the University of Groningen. Laboratory work and molecular analyses were supported by a grant from the Earth and Life Science Division of the Dutch Science Foundation (ARCHIMEDES project, 835.20.023) to GJH. This work was carried out within the frame of the 'Networks of Excellence' MarBef and EurOceans of the 6th Framework Program of the European Union. This work is in partial fulfilment of the requirements for a PhD degree from the University of Groningen by DDC.

## References

Ackermann HW, DuBow MS. (1987). Viruses of prokaryotes. In: *General Properties of Bacteriophages*. CRC, Boca Raton, FL, USA, Vol 1.

Allen EE, Bartlett DH. (2002). Structure and regulation of the omega-3 polyunsaturated fatty acid synthase genes from the deep-sea bacterium *Photobacterium profundum* strain SS9. *Microbiology* **148**: 1903–1913.

Allen EE, Facciotti D, Bartlett DH. (1999). Monounsaturated but not polyunsaturated fatty acids are required for growth of the deep-sea bacterium *Photobacterium profundum* SS9 at high pressure and low temperature. *Appl Environ Microbiol* **65**: 1710–1720.

Anderson MJ, Ford RB, Feary DA, Honeywill C. (2004). Quantitative measures of sedimentation in an estuarine system and its relationship with intertidal soft-sediment infauna. *Mar Ecol-Prog Ser* **272**: 33–48.

Aristegui J, Gasol JM, Duarte CM, Herndl GJ. (2009). Microbial oceanography of the dark ocean's pelagic realm. *Limnol Oceanogr* **54**: 1501–1529.

Avaniss-Aghajani E, Jones K, Chapman D, Brunk C. (1994). A molecular technique for identification of bacteria

using small subunit ribosomal RNA sequences. *BioTechniques* **17**: 144–149.

Borneman J, Triplett EW. (1997). Molecular microbial diversity in soils from eastern Amazonia: evidence for unusual microorganisms and microbial population shifts associated with deforestation. *Appl Environ Microbiol* **63**: 2647–2653.

Bouvier T, del Giorgio PA. (2007). Key role of selective viral-induced mortality in determining marine bacterial community composition. *Environ Microbiol* **9**: 287–297.

Breitbart M, Middelboe M, Rohwer F. (2008). Marine viruses: community dynamics, diversity and impact on microbial processes. In: Kirchmair DL (ed). *Microbial Ecology of the Oceans*. John Wiley & Sons Inc.: Hoboken, NJ, USA, pp 443–479.

Brussaard CPD. (2004). Optimization of procedures for counting viruses by flow cytometry. *Appl Environ Microbiol* **70**: 1506–1513.

Cardinale M, Brusetti L, Quatrini P, Borin S, Puglia AM, Rizzi A *et al*. (2004). Comparison of different primer sets for use in automated ribosomal intergenic spacer analysis of complex bacterial communities. *Appl Environ Microbiol* **70**: 6147–6156.

Danovaro R, Luna GM, Dell'Anno A, Pietrangeli B. (2006). Comparison of two fingerprinting techniques, terminal restriction fragment length polymorphism and automated ribosomal intergenic spacer analysis, for determination of bacterial diversity in aquatic environments. *Appl Environ Microbiol* **72**: 5982–5989.

De Corte D, Yokokawa T, Varela MM, Agogue H, Herndl GJ. (2009). Spatial distribution of Bacteria and Archaea and *amoA* gene copy numbers throughout the water column of the Eastern Mediterranean Sea. *ISME J* **3**: 147–158.

Del Giorgio PA, Bird DF, Prairie YT, Planas D. (1996). Flow cytometric determination of bacterial abundance in lake plankton with the green nucleic acid stain SYTO 13. *Limnol Oceanogr* **41**: 783–789.

DeLong EF. (1992). Archaea in coastal marine environments. *Proc Natl Acad Sci USA* **89**: 5685–5689.

DeLong EF, Preston CM, Mincer T, Rich V, Hallam SJ, Frigaard N-U *et al*. (2006). Community genomics among stratified microbial assemblages in the ocean's interior. *Science* **311**: 496–503.

Fisher MM, Triplett EW. (1999). Automated approach for ribosomal intergenic spacer analysis of microbial diversity and its application to freshwater bacterial communities. *Appl Environ Microbiol* **65**: 4630–4636.

Fuhrman JA. (1999). Marine viruses and their biogeochemical and ecological effects. *Nature* **399**: 541–548.

Fuhrman JA. (2000). Impact of viruses on bacterial processes. In: Kirchmair DL (ed). *Microbial Ecology of the Oceans*. Wiley-Liss Inc.: Hoboken, NJ, USA, pp 327–350.

Hammer Ø, Harper DAT, Ryan PD. (2001). PAST: paleontological statistics software package for education and data analysis. *Palaeontologia Electronica* **4**: 9 pp.

Hara S, Koike I, Terauchi K, Kamiya H, Tanoue E. (1996). Abundance of viruses in deep oceanic waters. *Mar Ecol Prog Ser* **145**: 269–277.

Herndl GJ, Agogue H, Baltar F, Reinthaler T, Sintes E, Varela MM. (2008). Regulation of aquatic microbial processes: the A 'microbial loop' of the sunlit surface waters and the dark ocean dissected. *Aquat Microb Ecol* **53**: 59–68.

Holmfeldt K, Middelboe M, Nybroe O, Riemann L. (2007). Large variabilities in host strain susceptibility and

- phage host range govern interactions between lytic marine phages and their *Flavobacterium* hosts. *Appl Environ Microbiol* **73**: 6730–6739.
- Kent AD, Jones SE, Yannarell AC, Graham JM, Lauster GH, Kratz TK *et al.* (2004). Annual patterns in bacterioplankton community variability in a humic lake. *Microb Ecol* **48**: 550–560.
- Kimmance SA, Wilson WH, Archer SD. (2007). Modified dilution technique to estimate viral versus grazing mortality of phytoplankton: limitations associated with method sensitivity in natural waters. *Aquat Microb Ecol* **49**: 207–222.
- Klieve AV, Bauchop T. (1988). Morphological diversity of ruminal bacteriophages from sheep and cattle. *Appl Environ Microbiol* **54**: 1637–1641.
- Larsen A, Castberg T, Sandaa RA, Brussaard CPD, Egge J, Heldal M *et al.* (2001). Population dynamics and diversity of phytoplankton, bacteria and viruses in a seawater enclosure. *Mar Ecol Prog Ser* **221**: 47–57.
- Lauro FM, Bartlett DH. (2008). Prokaryotic lifestyles in deep sea habitats. *Extremophiles* **12**: 15–25.
- Lee S, Fuhrman JA. (1987). Relationships between biovolume and biomass of naturally-derived marine bacterioplankton. *Appl Environ Microbiol* **53**: 1298–1303.
- Magagnini M, Corinaldesi C, Monticelli LS, De Domenico E, Danovaro R. (2007). Viral abundance and distribution in mesopelagic and bathypelagic waters of the mediterranean sea. *Deep-Sea Research Part I-Oceanographic Research Papers* **54**: 1209–1220.
- Marie D, Brussaard CPD, Thyraug R, Bratbak G, Vaulot D. (1999). Enumeration of marine viruses in culture and natural samples by flow cytometry. *Appl Environ Microbiol* **65**: 45–52.
- Moeseneder MM, Winter C, Arrieta JM, Herndl GJ. (2001a). Terminal-restriction fragment length polymorphism (T-RFLP) screening of a marine archaeal clone library to determine the different phylotypes. *J Microbiol Methods* **44**: 159–172.
- Moeseneder MM, Winter C, Herndl GJ. (2001b). Horizontal and vertical complexity of attached and free-living bacteria of the eastern Mediterranean Sea, determined by 16S rDNA and 16S rRNA fingerprints. *Limnol Oceanogr* **46**: 95–107.
- Murray AG, Jackson GA. (1992). Viral dynamics: a model of the effects size, shape, motion and abundance of single-celled planktonic organisms and other particles. *Mar Ecol Prog Ser* **89**: 103–116.
- Noble RT, Fuhrman JA. (1998). Use of SYBR Green I for rapid epifluorescence counts of marine viruses and bacteria. *Aquat Microb Ecol* **14**: 113–118.
- Ortmann AC, Lawrence JE, Suttle CA. (2002). Lysogeny and lytic viral production during a bloom of the cyanobacterium *synechococcus* spp. *Microb Ecol* **43**: 225–231.
- Pan LA, Zhang J, Zhang LH. (2007). Picophytoplankton, nanophytoplankton, heterotrophic bacteria and viruses in the Changjiang Estuary and adjacent coastal waters. *J Plankton Res* **29**: 187–197.
- Parada V, Sintes E, van Aken HM, Weinbauer MG, Herndl GJ. (2007). Viral abundance, decay, and diversity in the meso- and bathypelagic waters of the North Atlantic. *Appl Environ Microbiol* **73**: 4429–4438.
- Reinthal T, van Aken H, Veth C, Aristegui J, Robinson C, Williams PJLR *et al.* (2006). Prokaryotic respiration and production in the meso- and bathypelagic realm of the eastern and western North Atlantic basin. *Limnol Oceanogr* **51**: 1262–1273.
- Rohwer F. (2003). Global phage diversity. *Cell* **113**: 141–141.
- Sano E, Carlson S, Wegley L, Rohwer F. (2004). Movement of viruses between biomes. *Appl Environ Microbiol* **70**: 5842–5846.
- Simon M, Azam F. (1989). Protein content and protein synthesis rates of planktonic marine bacteria. *Mar Ecol Prog Ser* **51**: 201–213.
- Sullivan MB, Waterbury JB, Chisholm SW. (2003). Cyanophages infecting the oceanic Cyanobacterium *Prochlorococcus*. *Nature* **424**: 1047–1051.
- Suttle CA. (1999). Do viruses control the oceans? *Nat History* **108**: 48–51.
- Thingstad TF, Lignell R. (1997). Theoretical models for the control of bacterial growth rate, abundance, diversity and carbon demand. *Aquat Microb Ecol* **13**: 19–27.
- Thingstad TF. (2000). Elements of a theory for the mechanisms controlling abundance, diversity, and biogeochemical role of lytic bacterial viruses in aquatic systems. *Limnol Oceanogr* **45**: 1320–1328.
- Weinbauer MG. (2004). Ecology of prokaryotic viruses. *FEMS Microbiol Rev* **28**: 127–181.
- Weinbauer MG, Brettar I, Hofle MG. (2003). Lysogeny and virus-induced mortality of bacterioplankton in surface, deep, and anoxic marine waters. *Limnol Oceanogr* **48**: 1457–1465.
- Weinbauer MG, Rassoulzadegan F. (2004). Are viruses driving microbial diversification and diversity? *Environ Microbiol* **6**: 1–11.
- Wilhelm SW, Brigden SM, Suttle CA. (2002). A dilution technique for the direct measurement of viral production: a comparison in stratified and tidally mixed coastal waters. *Microbial Ecol* **43**: 168–173.
- Wilhelm SW, Suttle CA. (1999). Viruses and nutrient cycles in the sea—viruses play critical roles in the structure and function of aquatic food webs. *Bioscience* **49**: 781–788.
- Winget DM, Wommack KE. (2008). Randomly amplified polymorphic DNA PCR as a tool for assessment of marine viral richness. *Appl Environ Microbiol* **74**: 2612–2618.
- Winter C, Herndl GJ, Weinbauer MG. (2004a). Diel cycles in viral infection of bacterioplankton in the North Sea. *Aquat Microb Ecol* **35**: 207–216.
- Winter C, Moeseneder MM, Herndl GJ, Weinbauer MG. (2008). Relationship of geographic distance, depth, temperature, and viruses with prokaryotic communities in the eastern tropical Atlantic Ocean. *Microb Ecol* **56**: 383–389.
- Winter C, Smit A, Herndl GJ, Weinbauer MG. (2004b). Impact of virioplankton on archaeal and bacterial community richness assessed in seawater batch cultures. *Appl Environ Microbiol* **70**: 804–813.
- Winter C, Smit A, Herndl GJ, Weinbauer MG. (2005). Linking prokaryotic richness with viral abundance and prokaryotic activity. *Limnol Oceanogr* **50**: 968–977.
- Wommack KE, Ravel J, Hill RT, Chun JS, Colwell RR. (1999a). Population dynamics of Chesapeake bay virioplankton: total-community analysis by pulsed-field gel electrophoresis. *Appl Environ Microbiol* **65**: 231–240.
- Wommack KE, Ravel J, Hill RT, Colwell RR. (1999b). Hybridization analysis of Chesapeake Bay virioplankton. *Appl Environ Microbiol* **65**: 241–250.

Supplementary Information accompanies the paper on The ISME Journal website (<http://www.nature.com/ismej>)